Ion Runaway Instability in
Low-Density, Line-Driven Stellar-Winds

Stanley P. Owocki

Bartol Research Institute, University of Delaware
Newark, DE 19716 USA
owocki@bartol.udel.edu

Joachim Puls

Institut für Astronomie und Astrophysik der Universität München
Scheinerstraße 1, 81679 München, Germany
uh101aw@usm.uni-muenchen.de

ABSTRACT

We examine the linear instability of low-density, line-driven stellar-winds to runaway of the heavy minor ions when the drift speed of these ions relative to the bulk, passive-plasma of hydrogen and helium approaches or exceeds the plasma thermal speed. We first focus on the surprising results of recent steady-state, two-component models, which indicate that the limited Coulomb coupling associated with suprathermal ion drift leads not to an ion runaway, but instead to a relatively sharp shift of *both* the ion and passive fluids to a much *lower* outward acceleration. Drawing upon analogies with subsonic outflow in the solar wind, we provide a physical discussion of how this lower acceleration is the natural consequence of the weaker frictional coupling allowing the ion line-driving to maintain its steady-state balance against collisional drag with a comparitively shallow ion velocity gradient. However, we then carry out a time-dependent, linearized stability analysis of these two-component steady solutions, and thereby find that, as the ion drift increases from sub- to suprathermal speeds, a wave mode characterized by separation between the ion vs. passive-plasma goes from being strongly damped to being strongly amplified. Unlike the usual line-driven-flow instability of high-density, strongly-coupled flows, this ion separation instability occurs even in the long-wavelength, Sobolev limit, although with only modest spatial growth rate. At shorter wavelengths, the onset of instability occurs for ion drift speeds that are still somewhat below the plasma thermal speed, and moreover generally has a very large spatial growth. For all wavelengths, however, the *temporal* growth rate exceeds the already rapid growth of line-driven instability by a

typical factor of ~ 100, corresponding to the mass density ratio between the bulk plasma and the driven minor ions. We further show that this ion-separation mode has an inward propagation speed that is strongly enhanced (at its maximum by a similar factor of ~ 100) over the usual "Abbott-wave" speed of a fully coupled, line-driven flow, implying that in the context of this separation mode, the entire domain of any steady-state solution can be considered as 'subcritical'. Finally we note that, despite the extremely rapid linear growth rate, further analyses and/or simulations will be needed to determine whether the nonlinear evolution of this instabilty should lead to true ion runaway, or instead perhaps might be limited by damping from two-stream plasma instabilities.

1. Introduction

The winds from hot, luminous, massive stars are understood to be driven by the scattering of the star's continuum radiation by an ensemble of spectral-line transitions of heavy, minor ions (Lucy and Solomon 1970; Castor, Abbott, and Klein 1975, hereafter CAK; Abbott 1980, 1982; Pauldrach, Puls, and Kudritzki 1985). From even the initial considerations of this line-driving mechanism (McCrea 1935; Lucy and Solomon 1970; Lamers and Morton 1976; Castor, Abbott, and Klein 1976, hereafter CAK76), a key issue has been the degree to which the radiative momentum imparted to these heavy, minor ions could be shared through Coulomb collisions with the bulk mass of ionized hydrogen and helium, which have only a few strong line-transitions and thus, apart from cases with a near-zero metallicity (Kudritzki 2001; Bromm, Kudritzki and Loeb 2001), constitute a 'passive plasma' not much driven directly by radiation. Subsequent extensions of these early analyses [e.g., Springmann and Pauldrach 1992; Krticka and Kubat 2000, 2001 hereafter KK00 and KK01) generally confirm that, for the relatively dense winds from luminous OB stars, the collisional exchange is sufficient to keep the ions and bulk plasma tightly coupled, with the relative ion vs. bulk-plasma drift speed remaining well below the characteristic plasma thermal speed.

However, in the relatively low-density winds arising from lower-luminosity stars, e.g. main sequence B-type stars, the lower collision rate between the ions and passive plasma leads to a larger ion drift speed, in principle approaching or exceeding the plasma thermal speed. Because the cross-section for Coulomb collisions scales as the *inverse* fourth power of the microscopic relative velocity of the colliding particles, such a suprathermal drift has long been assumed to lead to an effective decoupling of the ions from the bulk plasma, a so-called "ion runaway" (Springmann and Pauldrach 1992; Babel 1995; Porter and Drew 1995).

Understanding the specifics of how this runaway should actually occur has proven, however, to be quite complicated. Springmann and Pauldrach (1992) showed that the friction associated with ion drift near the thermal speed could substantially heat the plasma; the associated rise in temperature and hence in thermal speed then also implies reduced collisional coupling, leading again to conditions for an expected ion runaway. If true runaway does occur, then the frictional heating is reduced, and so its net effect seems likely to be limited, causing only a moderately enhanced temperature for the bulk plasma, no more than a factor two or so above the stellar effective temperature. But if two-stream plasma instabililties were to damp the runaway and so effectively keep the ion drift within a few thermal speeds, then frictional heating could persist, leading to much higher temperatures, perhaps even high enough to be relevant for explaining the observed X-ray emission of many such B-type stars.

Again though, if true runaway does occur, it too could have varied consequences. For example, the much steeper ion velocity gradient implies that associated ion spectral-lines should become optically thin, thus limiting the maximum velocity inferred from wind-line absorption. Moreover, the rapid ion acceleration might even provide a source of moderately energetic particles into the interstellar medium. Finally, if the wind decoupling occurs before the passive-plasma outflow has reached escape speed, then this material could fall back onto the stellar surface (Porter and Skouza 1999).

Even setting aside questions of possible limitation of runaway by two-stream plasma instabilities, recent work raises questions whether ion runaway is indeed the expected outcome of even a simple multi-component model. Specifically, in a quite thought-provoking paper, KK00 derived, for the first time, quantitative velocity solutions for both the ions and passive plasma through a two-component extension of the usual single-fluid, CAK formalism for steady-state line-driven winds. For high-density winds they confirmed the standard CAK96 results of a strong, essentially single-fluid coupling between the minor ions and bulk plasma. But, quite surprisingly, for their case of a wind with moderately low density, they did *not* obtain solutions with ion runaway. Instead, as the collisional coupling becomes limited for suprathermal ion drift speeds, they found that *both* the ions and passive plasma simply shift to a lower-acceleration solution, with a relative ion flow speed that remains typically within a few thermal speeds of that for the bulk plasma.

This quite unexpected, seemingly unintuitive result raises several basic questions. First, what is the physical explanation for this turnover of both the ions and bulk plasma to a lower acceleration? Second, given the nonlinear nature of the fluid equations, might there be other solutions not uncovered in the KK00 analysis, including perhaps some characterized by ion runaway? Finally, and perhaps most importantly in the present context, what is the stability

of these slow-acceleration, steady-state solutions against time-dependent perturbations?

The goal of the present paper is to address these various questions, with particular focus on this issue of a possible fluid-type instability for ion runaway. Specifically, we provide a multi-component extension of the linear instability analyses carried out previously for single-fluid models of line-driven outflows (see, e.g., Owocki and Rybicki 1984, 1985 and references therein). These previous analyses show that such line-driven flows are generally highly unstable to small-scale perturbations with wavelength near or below the Sobolev length (over which the mean flow accelerates by an ion thermal speed). But in the long-wavelength, Sobolev limit, they yield marginally stable, radiative-acoustic wave modes that propagate inward relative to the flow at a fast characteristic speed, nowadays called the Abbott speed (Abbott 1980).

A key result of the analysis here is that, when the ion-drift speed exceeds the plasma thermal speed, even such long-wavelength, Sobolev-limit perturbations become unstable to a mode characterized by separation between the ions and bulk plasma. Moreover, compared to the single-fluid values, both the characteristic growth rate and the wave-propagation speed of this ion-separation mode are magnified by a large factor, of order 100, set by the mass-density ratio of the bulk plasma to minor ions. For long-wavelength perturbations, the fast propagation of the wave mode leads to only a modest spatial growth. But for short-scale perturbations, both the temporal and spatial growth can be very strong, with moreover an onset at moderately subthermal drift speeds. This suggests that, at least in the context of a linear perturbation analysis of multi-component model without yet accounting for any collective plasma effects, the KK00 steady-state solutions with slow ion acceleration should rapidly become disrupted by unstable wave modes leading to ion separation.

The organization of the remainder of this paper is as follows. We first lay the basis for our analysis by discussing how the general, time-dependent, two-component fluid equations (§2.1) reduce in the high-density, steady-state limit (§2.2) to the standard single-fluid CAK formalism, focussing in particular (§2.3) on the possibility of alternate, slow-acceleration solutions in the CAK model. We next (§2.4) derive a scaling analysis for the general conditions (e.g., wind mass loss rate, stellar gravity) under which the ion drift speed can be expected to approach the plasma thermal speed. We then (§2.5) discuss the KK00 model for steady-state outflow of a two-component flow, focussing on the physical reasons for the shift to slow-acceleration under conditions of suprathermal ion drift. With this basis, we finally present (§3.1) our linear perturbation analysis, showing that solutions with suprathermal drift are unstable to even long-wavelength perturbations (§3.2), and that short-wavelength perturbations have strong spatial growth even for mildly subthermal ion drift (§3.3). We conclude (§4) with a brief summary and outlook for future work.

2.   Two-Component, Line-Driven Stellar Wind

2.1.   Time-Dependent Equations of Motion

Let us begin with the general, time-dependent forms of the relevant equations of motion for a line-driven flow. Under the standard assumption of a 1D, radial (e.g., spherically symmetric) outflow, consider a two-component wind consisting of line-driven minor ions (i) that interact via Coulomb collisions with a passive plasma (p) consisting of the hydrogen and helium that represent the bulk of the plasma mass. The time-dependent equations of motion for each component are of the form

$$\frac{\partial v_p}{\partial t} + v_p \frac{\partial v_p}{\partial r} = -g + \frac{1}{\rho_p} R_{pi} \tag{1}$$

and

$$\frac{\partial v_i}{\partial t} + v_i \frac{\partial v_i}{\partial r} = -g - \frac{1}{\rho_i} R_{pi} + g_i, \tag{2}$$

where t is the time, r is the radius, g is the effective gravitational acceleration (corrected for Thomson scattering by free electrons), g_i is the radiative line-acceleration on the ions, and the $v_{p,i}$ and $\rho_{p,i}$ are the velocities and densities of the passive plasma and ions, with typically $\rho_p \approx 100\rho_i$ for solar abundances.

Note that we have ignored the gas pressure of both components, as this plays little direct role in the acceleration of such a line-driven stellar wind. Moreover, for simplicity, and in conjunction with the initial KK00 analysis, we also avoid here an explicit treatment of the respective plasma energy equations, and assume instead that both the ion and bulk plasma remain at a common, constant temperature, corresponding roughly to the stellar effective temperature. We thus defer to future work consideration of the frictional heating that was described originally by Springmann and Pauldrach (1992), and analyzed further in the recent follow-up paper by KK01.

The force-per-unit-volume for the collisional coupling between the ions and passive plasma is of the form (Springmann and Pauldrach 1992; KK00),

$$R_{pi} = n_p n_i k_{pi} G(x_{pi}), \tag{3}$$

where $n_{p,i}$ are the corresponding number densities of each component, and

$$k_{pi} = \frac{4\pi \ln \Lambda Z_p^2 Z_i^2 e^4}{kT} \frac{v_i - v_p}{|v_i - v_p|} \tag{4}$$

with k Boltzmann's constant, $Z_{p,i}$ the mean atomic charges for each component in units of the electronic charge e, and, as noted above, we have assumed, for simplicity, a fixed,

common temperature T for both components. The Coulomb logarithm is given by (Lang 1974)

$$\ln \Lambda = \ln \left[\frac{24\pi}{\sqrt{n}} \left(\frac{kT}{4\pi e^2} \right)^{3/2} \right],$$

(5)

where $n = n_p + n_i + n_e$ is the total number density of free particles.

The collisional coupling depends on the ion-separation drift-speed relative to the passive plasma, measured here in units of a mass-weighted thermal speed,

$$x_{pi} \equiv \frac{|v_i - v_p|}{v_{th} \sqrt{1 + A_i/A_p}},$$

(6)

where $v_{th} = \sqrt{2kT/A_i m_a}$ is the ion thermal speed, m_a is the atomic mass unit, and A_p and A_i are the mean atomic mass numbers for passive plasma and ions. When integrated over the thermal distributions, the collisional dependence on ion drift enters through the "Chandrasekhar function", which is plotted in figure 1 and is defined by

$$G(x_{pi}) \equiv \frac{\Phi(x_{pi})}{2x_{pi}^2} - \frac{e^{-x_{pi}^2}}{2\sqrt{\pi}},$$

(7)

where Φ is the error function (Dreicer 1959). At small ion-drift-speeds, the collisional coupling increases linearly with ion drift, with the Chandrasekhar function approximated by

$$G(x_{pi}) \approx \frac{2\,x_{pi}}{3\sqrt{\pi}} \quad ; \quad x_{pi} \ll 1 .$$

(8)

However, at suprathermal ion-drift-speeds $x_{pi} > 1$, the decline of the Coulomb cross-section at large relative collision speeds leads to a net decrease in the overall coupling, with the Chandraskhar function taking on the asymptotic form,

$$G(x_{pi}) \approx \frac{1}{2x_{pi}^2} \quad ; \quad x_{pi} \gg 1 .$$

(9)

The maximum value $G_{max} = 0.214$ occurs at the scaled drift speed $x_{pi} = 0.968$, that is, near, but not exactly at, a thermal-speed ion-drift, $x_{pi} = 1$ (figure 1).

2.2. Steady-State Form

Let us first consider wind solutions for the case of a steady, time-independent flow, for which the eqns. (1) and (2) become

$$v_p \frac{\partial v_p}{\partial r} + g = \frac{1}{\rho_p} R_{pi}$$

(10)
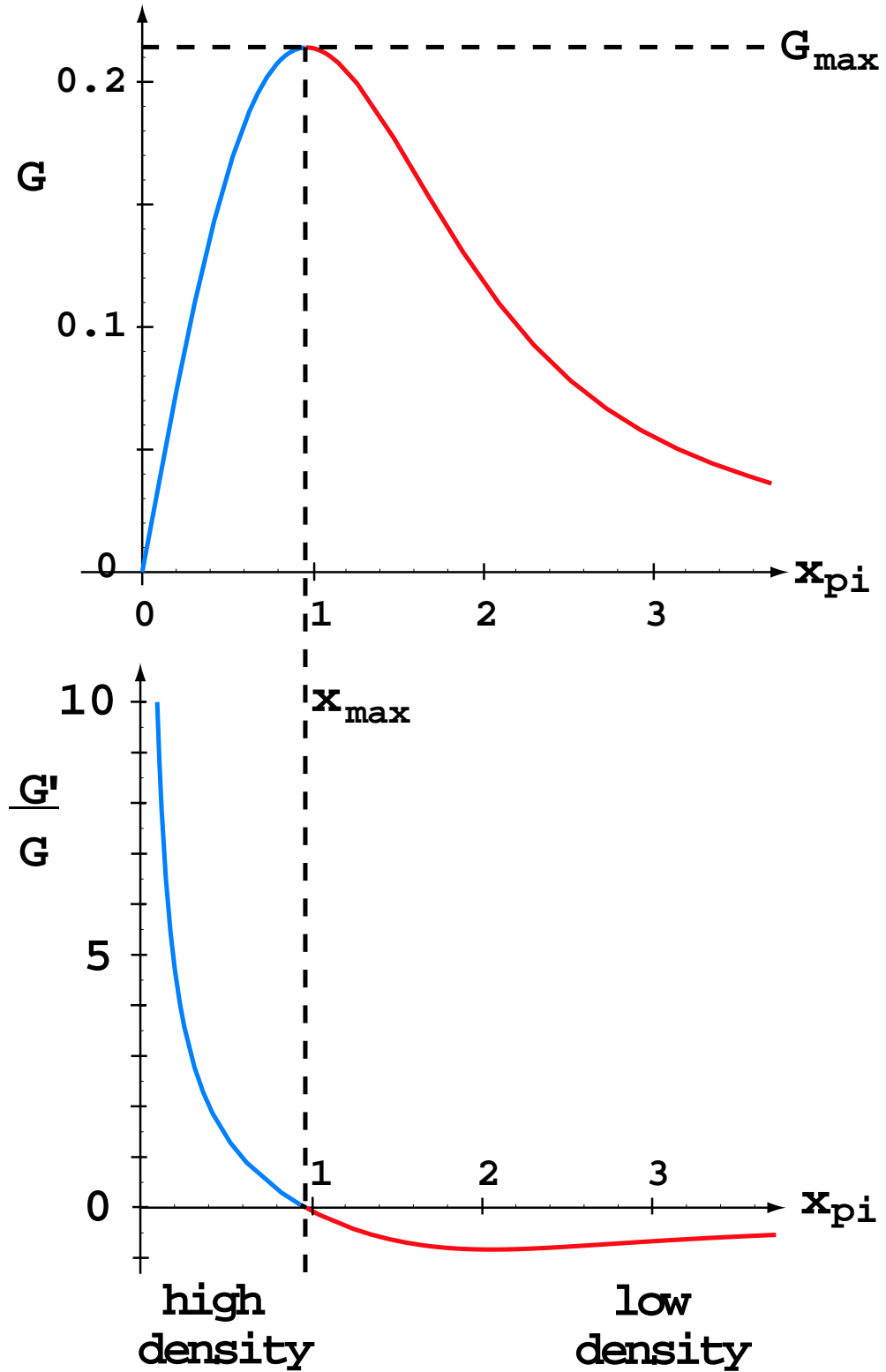
Fig. 1.— The Chandrasekhar function, $G(x_{pi})$ (top), and its logarithmic derivative, $G'(x_{pi})/G(x_{pi})$ (bottom), plotted vs. the thermally scaled ion-drift speed x_{pi} [defined in eqn. (6)].

and

$$v_i \frac{\partial v_i}{\partial r} + g + \frac{1}{\rho_i} R_{pi} = g_i. \tag{11}$$

Here we've separated onto the left and right sides the terms that tend to retard or promote a positive, outward acceleration for each component. Since the only external source of momentum to propel such an outward acceleration is the radiative line-force imparted to the ions, these ions clearly must drift faster than the passive component. Thus the frictional coupling is a retarding term for the ions, but is the essential accelerating term for the passive plasma.

A further key distinction stems from the generally much larger mass-density of the passive plasma, with typical ratio $\rho_p/\rho_i \sim 100$. This implies a similar difference factor in the accelerations for the collisional drag on the ions versus collisional push on the passive plasma. As such, apart from a fully developed ion runaway, both the ion inertia and gravity term should be ignorable in comparison to the frictional drag on the ions, thus implying that the principal momentum balance for the ions is between this drag and the line-force,

$$R_{pi} \approx \rho_i g_i. \tag{12}$$

Applying this in equation (10) we obtain

$$v_p \frac{\partial v_p}{\partial r} + g = \frac{\rho_i}{\rho_p} g_i. \tag{13}$$

2.3. The CAK Model for Single-Fluid Outflow

Within the CAK formalism for line-driving, the ion line-force depends itself on the ion acceleration, i.e. $g_i \sim (v_i \, dv_i/dr)^\alpha$, where α is the usual CAK power-index for the line-opacity distribution. To recover the standard CAK equation of motion, one thus must further assume a close coupling between the ion and passive-plasma flow speeds, i.e. $v_i \approx v_p$, which thus also implies a closely coupled acceleration, $v_i \, dv_i/dr \approx v_p \, dv_p/dr \equiv v \, dv/dr$. Under these conditions, the right side of eqn. (13) becomes the CAK line-force,

$$\frac{\rho_i}{\rho_p} g_i = g_{cak} \sim \frac{1}{r^2} \left(\frac{1}{\rho} \frac{dv}{dr} \right)^\alpha. \tag{14}$$

This expression thus now makes quite explicit that the uncoupled ion driving is a factor $g_i/g_{cak} = \rho_p/\rho_i \approx 100$ stronger than the usual CAK line-force.

Using the equation of mass continuity to solve for the plasma density $\rho = \dot{M}/4\pi v r^2$ in terms of the mass loss rate $\dot{M}$, we find we can write the CAK equation of motion in the

scaled, dimensionless form

$$w + 1 = fCw^{\alpha}, \tag{15}$$

where $w \equiv v(dv/dr)/g$ is the flow acceleration in units of the local gravity, and the flow constant $C \sim k_{cak}L_*/(\dot{M}^{\alpha}M_{eff}^{1-\alpha})$ depends on the stellar luminosity L_*, the CAK line-driving normalization parameter k_{cak}, the mass loss rate $\dot{M}$, and the effective stellar mass M_{eff} (corrected for Thomson acceleration).

2.3.1. The role of the finite-disk correction factor in steep wind acceleration

The factor f corrects the original CAK 'point-star' approximation to take account of the finite angular extent of the stellar core (Friend and Abbott 1986; Pauldrach, Puls, and Kudritzki 1986). In general, this factor depends itself in a rather complex way on the velocity and its gradient. It typically begins at a value $f_* \approx 1/(1+\alpha)$ near the stellar surface, and then increases outward, past unity at the point where the wind has a locally isotropic expansion (with $dv/dr = v/r$), then eventually falling back to unity at large radii, where the star is indeed well approximated by a point-source.

Following broadly the insightful analysis given by Gayley (2000), let us seek a conceptual understanding of the CAK solution that will also prove helpful in interpreting the two-component results of KK00. In particular, let us ignore the complex velocity dependence of this finite-disk factor and consider simply the nature of solutions to eqn. (15) assuming a prescribed, fixed stratification of f. Figure 2 shows a graphical solution for various values of the constant C, corresponding to various choices of the mass loss rate $\dot{M}$. For high $\dot{M}$, there are no solutions, while for low $\dot{M}$, there are two solutions. The two limits are separated by a critical case with one solution – corresponding to the *maximal* mass loss rate – for which the function fCw^{α} intersects the line $1 + w$ at a tangent. For this critical case, the tangency requirement implies $\alpha f_c C_c w_c^{\alpha-1} = 1$, which together with the original equation (15) yields the critical value $C_c = 1/[f_c\alpha^{\alpha}(1 - \alpha)^{1-\alpha}]$. Moreover, since inclusion of the finite-disk-correction factor results in a rather low-lying critical point (Friend and Abbott 1986; Pauldrach et al. 1986), the severest constraint on maintaning this mass loss rate occurs near the stellar surface, where the finite disk correction factor has its minimum value $f_c = f_* = 1/(1 + \alpha)$. This then fixes the critical value of $C_c = (1 + \alpha)/[\alpha^{\alpha}(1 - \alpha)^{1-\alpha}]$ (which through the dependence $C \sim \dot{M}^{-\alpha}$ thereby fixes the finite-disk-modified, CAK mass-loss-rate).

For such critical solutions, the CAK equation of motion (15) at other locations generally away from the critical point becomes

$$w + 1 = \left[\frac{(1 + \alpha)}{\alpha^{\alpha}(1 - \alpha)^{1-\alpha}} \right] f\, w^{\alpha}. \tag{16}$$
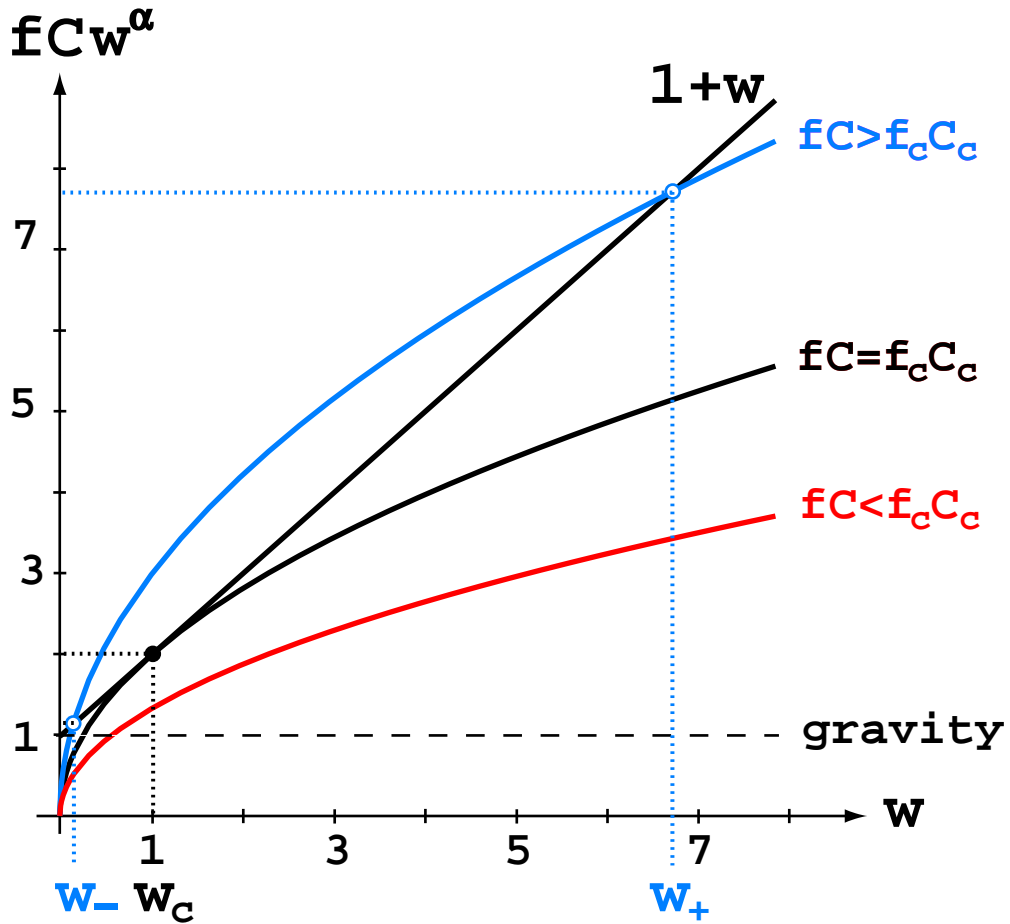
Fig. 2.— Graphical solution of the CAK equation of motion, showing cases with 0, 1, or 2 solutions depending of the value of fC, where f is the finite disk correction factor, and $C \sim 1/\dot{M}^\alpha$. Specifically the plot here assumes $\alpha = 1/2$, and curves with 2 and 0 solutions have fC values that are a factor 1.5 above and below the critical, single-solution case with $f_c C_c = (1 + \alpha)/\left[\alpha^\alpha (1 - \alpha)^{1-\alpha}\right]$.

As a specific example, let us examine the case $\alpha = 1/2$, for which the term in square brackets is 3, and eqn. (16) reduces to a simple quadratic equation in $\sqrt{w}$, with solutions

$$\sqrt{w_\pm} = \frac{3}{2}f\left(1 \pm \sqrt{1 - 4/9f^2}\right). \qquad (17)$$

The critical acceleration in this case occurs when $f = 2/3$, for which $w_c = w_+ = w_- = 1$. Note, however, that as f increases from this initial, critical value, there develop two quite distinct solutions for the acceleration w; these are plotted in figure 3 on a semi-log scale over the range $2/3 < f < 1.2$. Beyond the critical point, the standard, single-fluid CAK model typically follows the w_+ branch.[1]

Thus, as f increases outward from its critical value near the stellar surface, we see from figure 3 that this steeper solution can lead to a substantially stronger acceleration in the outer wind. For example, at the point of isotropic wind expansion, where $dv/dr = v/r$ and so $f = 1$, we find $w_+ = ((3 + \sqrt{5})/2)^2 \approx 6.9$, implying that the outward wind acceleration at this point is this substantial factor larger than the local, inward acceleration of gravity. As discussed by Gayley (2000), it is this 'leveraging' of the finite-disk correction factor that leads to terminal wind speeds of such corrected CAK models being a factor of ~ 3 times the surface escape speed; in contrast, the point-star CAK model in this case would predict $v_\infty/v_{esc} = \sqrt{\alpha/(1 - \alpha)} = 1$. This factor 3 above the escape speed thus implies that the work done by the line-force against inertia is a factor ~ 9 times that done against gravity, leading to what Gayley (2000) calls the 'weak-gravity' perspective for understanding hot-star winds.

This 'leveraging' of the finite-disk factor f is even stronger when comparing the ratio of the steep vs. shallow flow solutions; for example, $w_+/w_- = \left[3 + \sqrt{5})/4\right]^4 \approx 47$ for $f = 1$, and for only slightly larger values of f, we see from figure 3 that these two solutions can differ by more than two orders of magnitude. Physically, this means that, in addition to the rapidly accelerating, steep-slope solution that is usually followed in the outer part of a finite-disk-corrected CAK wind, the flow also has available, as a kind of 'backup', a solution with a much lower acceleration, in which the outward driving now mainly just needs to overcome the retarding effect of gravity, instead of the much stronger inertia associated with a rapid acceleration.

---

[1]Feldmeier and Shlosman (2001) have recently discussed how maintaining an outflow along the shallow-slope, w_- solution requires in this single-fluid model a special kind of outer boundary condition. (Note also that these authors use the term 'runaway' to mean the rather abrupt shift that can occur from shallow to steep solutions.)
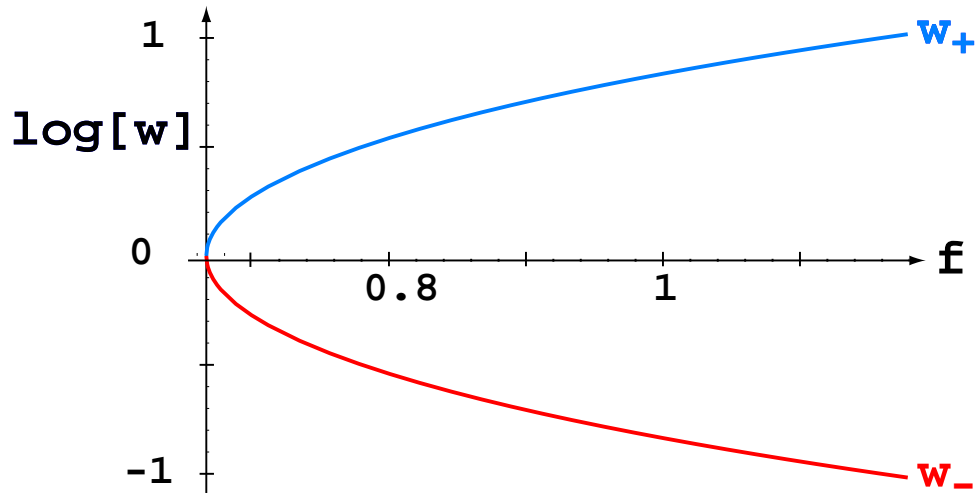
Fig. 3.— Log of the gravity-scaled flow acceleration for steep (w_+) and shallow (w_-) solutions, plotted vs. the finite disk correction factor f for critical, CAK solutions with power index $\alpha = 1/2$.
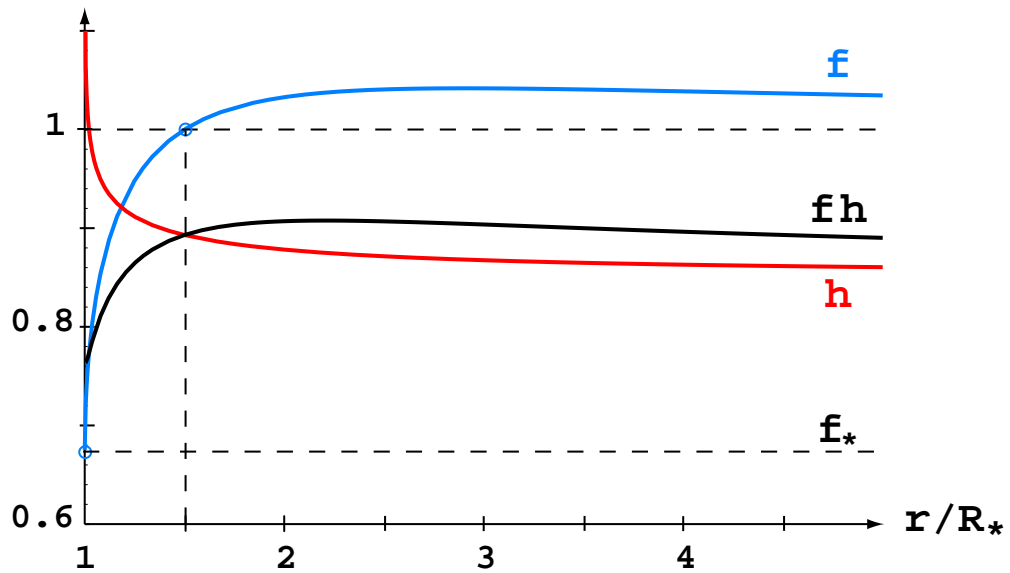
Fig. 4.— Comparison of the radial variations of the finite-disk correction factor $f(r)$, the ionization correction factor $h(r)$ for $\delta = 0.1$, and their product $h(r)f(r)$, assuming a 'beta' velocity law $v(r) = v_\infty(1 - R_*/r)^\beta$, taking here $\beta = 1/2$.

2.3.2. The role of an ionization-correction factor in reducing wind acceleration

As we shall discuss further below (§2.5), this 'backup solution' provides an important key to understanding the KK00 two-component solutions with an abrupt shift to lower acceleration. However, to facilitate an accurate analysis of the specific solution shift found by KK00, we need to consider one further effect that they included, namely the reduction in line-force associated with the shift in wind ionization, as parameterized by the ionization correction factor (Abbott 1982),

$$h(r) \sim \left[\frac{n_e}{W} \right]^{\delta}, \tag{18}$$

where n_e is the electron density, the exponent has a typical value $\delta \approx 0.1$, and $W = 0.5(1-\mu_*)$ is the core-radiation dilution-factor, with $\mu_* \equiv \sqrt{1 - R_*^2/r^2}$. Using the mass-continuity equation, the radial variation of this ionization correction can be written as

$$h(r) = \left[(1 + \mu_*(r)) \frac{v_c}{v(r)} \right]^{\delta}, \tag{19}$$

where we have normalized to have $h(r_c) \equiv 1$ at the critical point radius $r_c \approx R_*$, with critical velocity $v_c = v(r_c)$. As illustrated in figure 4, this is a decreasing function of radius, and as such acts to counter the outward increase in line-driving associated with the finite-disk correction. Thus, to take account of these ionization effects in the above analysis of the steepness of wind solutions, we can simply replace the f with hf in eqns. (15)-(17). The net upshot is that appropriate values of hf are smaller, thus implying somewhat weaker values for the gravity-scaled acceleration w_+. This is generally consistent with the lower wind accelerations and lower wind terminal speeds found in such models with a non-zero δ. In the present context, it will moreover prove relevant to explaining the details of the slope-shift in the KK00 two-component models, as we shall now see.

2.4. Conditions for Thermal-Speed Drift and Maximal Coupling

Let us thus return to a two-component model in which, as given in eqn. (10), the passive plasma is accelerated against its retarding inertia and gravity by the outward force from collisions with faster drifting ions. Making use of the definitions for the dimensionless acceleration w and for the collisional coupling term R_{pi} [eqn. (3)], we may rewrite eqn. (10) in the form

$$g(1 + w) = \frac{k_{pi}}{A_p A_i m_a^2} \rho_i G(x_{pi}). \tag{20}$$

The ion drift yields its maximum possible coupling at the scaled drift speed $x_{pi} = 0.968$, where the Chandrasekhar function has its maximum value $G_{max} = 0.214$. We then solve

eqn. (20) for the passive-plasma density at which this maximal coupling would occur,

$$\rho_{max} \approx \left[\frac{(1+w)g\,kT}{y}\right]\left[\frac{A_p^2 m_a^2}{4\pi\,G_{max}\ln\Lambda\,Z_p^2 Z_i^2 e^4}\right], \tag{21}$$

where $y \equiv (A_p/A_i)(\rho_i/\rho_p) = n_i/n_p$ is the relative ion number abundance. Alternatively, for a given mass loss rate $\dot{M}$, we can convert this to an estimate of the wind velocity at which such maximal coupling would occur,

$$
\begin{aligned}
v_{max} &\approx \left[\frac{\dot{M}\,y}{(1+w)GM\,kT}\right]\left[\frac{G_{max}\ln\Lambda\,Z_p^2 Z_i^2 e^4}{A_p^2 m_a^2}\right] & (22)\\
&\approx 560\,\text{km/s}\left[\frac{\dot{M}_{-11}\,y_{-3}}{M_1 T_4}\right]\left[\frac{2}{1+w}\right]\left[\frac{Z_i}{2}\right]^2. & (23)
\end{aligned}
$$

In the latter equality, we have assumed the specific parameter values $\ln\Lambda = 20$, $A_p \approx 1$, and $Z_p \approx 1$, with the scaled quantities defined by $\dot{M}_{-11} \equiv \dot{M}/(10^{-11}M_\odot/yr)$, $T_4 \equiv T/10^4 K$, $M_1 \equiv M/10^1 M_\odot$, and $y_{-3} \equiv y/10^{-3}$.

As an example, consider the low-density, B5-star wind computed by KK00. From their figure 2, we see that this model reaches collisional maximum at $r \approx 1.3R_*$, where the outflow velocity is $v \approx 350$ km/s. By comparison, applying their stellar parameters – $M_1 = .436$, $T_4 = 1.55$, $\dot{M}_{-11} = 4.8$, $Z_i = 2$, and $y_{-3} = 1.06$ – we find that eqn. (23) yields for this model $v_{max} \approx (420\,\text{km/s})\,(2/(1+w))$. From KK00 figure 2, we can estimate an inner wind acceleration factor $w \approx 2$, which thus predicts $v_{max} \approx 280$ km/s, only slightly below KK00's computational result. In the simple analysis given above, such an acceleration would occur for $hf \approx 0.71$, which seems a reasonable value for the combined effect of the ionization and finite-disk correction factors.

This generally good agreement with such a detailed numerical calculation thus demonstrates that eqn. (23) provides a quite useful, simple analytic formula for predicting the required wind conditions for thermal-speed drift and the associated maximum in collisional coupling. In particular, it shows that there is only a limited range of wind parameters, e.g. mass loss rate, over which such a collisional maximum should occur within the wind. Namely, when this maximal velocity is greater than the wind terminal speed, $v_{max} > v_\infty$, then throughout the entire wind the velocity should simply follow the standard, single-fluid solution for a finite-disk-modified CAK model. Moreover, when the maximal velocity is estimated to be less than the CAK critical velocity, $v_{max} < v_c$, then one can expect a fully decoupled solution, as derived by Babel (1995) for very low-density winds. Since typically $v_\infty/v_c \approx 10$, this suggests that maximal coupling within the wind should be limited to a similar, factor 10 range of mass loss rates, i.e. within an order of magnitude of $\dot{M} \approx 10^{-11}M_\odot/\text{yr}$,

assuming that the scaled abundance, mass, and temperature in eqn. (23) are likewise are also of order unity.

2.5.   Slow-Acceleration Solutions for Flows Beyond Maximal Coupling

With this background, let us next consider more carefully these cases for which $v_c < v_{max} < v_\infty$, and specifically examine the reasons for the shift to slow acceleration solutions. Our aim is to supplement the mathematically formal, Taylor-expansion analysis given by KK00 [See their eqns. (22)-(25).] with a more physically intuitive discussion.

2.5.1.   Physical reasons for slow acceleration vs. ion runaway

As ion drift becomes suprathermal, the collisional coupling set by $R_{pi} \sim G(x_{pi})$ drops sharply, as $\sim 1/x_{pi}^2$ in the high-drift-speed limit $x_{pi} \gg 1$. (See eqn. (9) and figure 1 here, and also figure 3 of KK00.) As noted in the introduction, most previous analyses had anticipated that such a drop in collisional coupling would lead to an ion runaway. The intuitive expectation for this appears based on our everyday experience that the harder one pushes on something, the faster it will accelerate. But hidden in the application of this general notion to the case of ion acceleration are two assumptions: first that the reduction in frictional drag on the ions would lead to a stronger net outward force, in effect assuming that the line-force would remain the same; and second, that this stronger net ion force would act against ion inertia to enhance the ion acceleration.

But as already discussed in §2.3, in the steady-state, coupled flow acceleration leading up to the collisional coupling maximum, the ion line-force is *not* balanced against ion *inertia*, but rather, as given in eqn. (12), against the collisional drag from the passive plasma. Thus, when this collisional drag is reduced, the natural steady-state response of the ions is simply to proportionately reduce the ion line-force, which accordingly implies a lower ion velocity gradient. As such we thus see that a key fallacy in the expectation of a steady-state ion runaway is that the line-driving would simply remain fixed, and not, as occurs in the KK00 model, reduce itself in accord with the lower collisional drag it is balancing.

Of course, this reduced collisional force also means that the passive plasma can no longer be maintained along the steeper slope acceleration; but with the 'backup' of the lower-slope solution discussed above, the protons can still be maintained in a positive, albeit slow acceleration, with the weaker collisional driving now acting primarily to overcome gravity,

not inertia. This implies a passive-plasma momentum balance [cf. eqn. (20)] given by

$$g \approx \frac{k_{pi}}{A_p A_i m_a^2} \frac{\rho_i}{2x_{pi}^2} \,, \tag{24}$$

where we've used the large-drift-speed limit for the Chandrasekhar function, eqn. (9). Taking the ratio of eqns. (24) and (20), and applying the latter along a steep acceleration w_+ that leads up to the maximum in collisional coupling, we find the post-maximum drift must satisfy

$$x_{pi} \approx \sqrt{(1+w_+)/2G_{max}} = 1.53 \sqrt{1+w_+} \,. \tag{25}$$

Since typically $w_+ \approx 2$, we see that collisional coupling of ions to the passive plasma is maintained at drift speeds that are $x_{pi} \approx 2.6$ times the thermal speed. Note here that the *post*-maximum suprathermal ion drift depends on the *pre*-maximum passive-plasma acceleration, since the latter helps determine the density at which this maximum is reached. There is no tendency for any ion runaway because the assumption of a steady, continuous solution across this maximum coupling ensures that, if the pre-maximum acceleration is increased, it simply requires a somewhat larger post-maximum ion drift. Overall, the situation is thus that *both* the ions and passive plasma turn over to such a shallow outward acceleration, as was found in the two-component flow solutions computed by KK00.

2.5.2. Subcritical nature of ion outflow and analogy with the subsonic solar wind

This circumstance of a reduced retarding force leading to a lower, not higher, outward acceleration is somewhat analogous to what occurs in the subsonic portion of a pressure-driven outflow, like the solar wind. In this subsonic region, the primary momentum balance is not that of the outward gas pressure against inertia, but rather a nearly hydrostatic balance of gas-pressure-gradient force against gravity. If one now imagines applying some new, outward, body force, then in effect the net gravity is reduced, and so the hydrostatic balance can be maintained with a *smaller* pressure gradient. This generally implies a smaller density gradient, which in turn through the mass continuity relation for a steady flow ($\rho \sim 1/v$), also implies an accordingly smaller velocity gradient. The net result is thus that an *increased* outward force leads to a *lower* outward flow acceleration. [For further discussion of these general points, see, e.g., Leer and Holzer (1980), and Lamers and Cassinelli (1999).]

This analogy with the subsonic portion of a pressure-driven wind suggests that the behavior of such a two-component line-driven wind must in some ways be considered 'sub-critical', even though the coupled flow has already passed the CAK critical point. As first discussed by Abbott (1980), the critical point of a CAK wind can be considered quite analogous to the sonic point of a pressure-driven wind if one takes into account the effect of

radiation in modifying the restoring force for perturbations. Just as the sonic point in a pressure-driven wind represents a point beyond which sound waves can no longer propagate back to the wind base, there exists in a line-driven wind a radiatively modified sound wave, nowadays called an Abbott wave, which likewise can no longer propagate inward beyond the CAK critical point.[2]

In the context of the effectively subcritical behavior of the two-component models, this suggests the existence of a 'fast ion-mode Abbott' wave, applicable to wave propagation for ions that are not fully coupled to the bulk plasma (KK01). To discern such wave modes, it is necessary now to carry out a linearized perturbation analysis of the two-component fluid equations.

In this context, it seems appropriate to emphasize here that the above physical explanations for the slow-acceleration solutions are completely grounded in the inherent *assumption* of a *steady-state* outflow. In particular, these arguments do not guarantee the physical *stabilty* of such steady-state solutions. As we shall now see, when one includes the possibility of intrinsic time-variability within a linearized perturbation analysis, the original intuitive expectation that an increasing line-force could instead work to overcome ion inertia rears back with a vengeance, leading to a very strong linear instability that may well completely disrupt such steady, slow accelerations, and lead indeed to a rapid ion runaway.

3.   Time-Dependent Perturbation Analysis

3.1.   Two-Component Equations for Linear Sinusoidal Perturbations

Let us thus now consider the stability of a steady-state ($\partial/\partial t = 0$), two-component, coupled flow with nearly equal ion and passive-plasma velocities ($v_p \approx v_i$) and accelerations $v_p dv_p/dr \approx v_i dv_i/dr$. Applying then small-amplitude, sinusoidal velocity perturbations of the form $\delta v_{p,i} \sim e^{i(kr-\omega t)}$ to the ion and passive-plasma equations of motion (1) and (2), the corresponding linearized, first-order, perturbation equations take the form,

$$-i\omega\delta v_p - \frac{b}{\rho_p}(\delta v_i - \delta v_p) = 0 \qquad (26)$$

---

[2]   The reader should be cautioned here that there exists considerable uncertainty as to the physical relevance of such Abbott waves; Owocki and Rybicki (1986) applied a Green's function analysis to show, for example, that in a simple pure-absorption model such Abbott waves cannot, in fact, carry inward information faster than an *ordinary* sound wave. However, recent work, e.g. by Owocki and Puls (1999), suggests that line-scattering effects may allow a physical information transport that might be appropriately modelled in terms of such Abbott waves.

and

$$-i\omega \delta v_i + \frac{b}{\rho_i}(\delta v_i - \delta v_p) - \left(\frac{\delta g_i}{\delta v_i}\right) \, \delta v_i = 0, \tag{27}$$

where b is the perturbed collisional coupling term, and $\delta g_i / \delta v_i$ is the perturbed ion line-acceleration, both of which are described in greater detail below.

These equations apply in a frame with stellar velocity $v \approx v_p \approx v_i$ that is nearly comoving with both the passive-plasma and ion mean flows, and thus advection terms proportional to $v_{p,i} \, ik\delta v_{p,i}$ have vanished. We further assume here a WKB approach, whereby variations in the mean wind are assumed to have a scale $v/v' \gg 1/k$ that is much larger than the perturbation wavelength, thus allowing also neglect of terms proportional to mean-wind velocity gradients $v'_{p,i}$. Finally, note that, for simplicity, we are focusing here only on the effect of perturbations in velocity $\delta v_{p,i}$, ignoring, for example, associated perturbations in density $\delta \rho_{p,i}$. Justification for this approximation is given in the Appendix.

The perturbed collisional coupling term is given by

$$\begin{aligned}
b &\equiv \frac{R'_{pi}(x_{pi})}{v_{th} \, \sqrt{1 + A_i/A_p}} \\
&\approx \left[\frac{1}{\alpha\sqrt{1 + A_i/A_p}} \frac{G'(x_{pi})}{G(x_{pi})}\right] \left[\frac{\alpha \, g_{cak}}{v_{th}}\right] \rho_p \\
&\equiv q(x_{pi}) \, \Omega \, \rho_p,
\end{aligned} \tag{28}$$

where the primes denote differentiation. In the second equality here we have used eqns. (12) and (14), which relate the CAK line-force g_{cak} to the collisional rates for this assumed case of a still-coupled mean flow, and have noted that the logarithmic derivative R'_{pi}/R_{pi} can simply be replaced by the corresponding derivative of the Chandrasekhar function, G'/G. The last equality implicitly defines symbols for the two bracketed factors. The Ω represents a characteristic rate, roughly equal to the growth rate for the line-driven instability in the single fluid case [cf. eqn. (52) of Owocki and Rybicki (1984)].

The q is a dimensionless, collisional coupling strength that is just directly proportional to the logarithmic derivative of the Chandrasekhar function (figure 1). In all computations here, we will assume a fixed proportionality constant such that

$$q(x_{pi}) = \frac{1}{2} \frac{G'(x_{pi})}{G(x_{pi})}, \tag{29}$$

which is roughly appropriate for typical parameter values, e.g. $\alpha = 1/2$ and $A_i/A_p = 15$. In the analysis below (§§3.2-3.3), the dependence of this collisional coupling strength on the ion drift speed x_{pi} will play a key role in determining the stability of perturbation eigenmodes. (See, e.g., figures 5-7.)

3.2.   Analysis for Long-Wavelenth Perturbations

3.2.1.   Perturbed line-force in the Sobolev limit

For the perturbed ion line-force δg_i, we consider two approximations. First, following Abbott (1980), we assume that, like the mean force, the perturbed force simply scales with the velocity gradient, $\delta g \sim \delta v' \sim ik\delta v$; such a form applies in the limit that the perturbation wavelength $\lambda = 2\pi/k$ is much larger than the Sobolev length $L \equiv v_{th}/v'$, over which the mean flow accelerates by an ion thermal speed v_{th}. A second, more general form, which applies for arbitrary wavelength perturbations, is analyzed in the next section (§3.3).

In the present context of the line-force on the minor ion component, this Sobolev limit form gives

$$
\begin{aligned}
\frac{\delta g_i}{\delta v_i} &= \frac{\delta v_i'}{\delta v_i}\frac{\partial g_i}{\partial v_i'} \\
&= ik\,\frac{\alpha g_i}{v_i'} \\
&= ik\,U_i \\
&= ik\,U\,\frac{\rho_p}{\rho_i} \\
&= ikL\,\Omega\,\frac{\rho_p}{\rho_i} \\
&= ikL\,\Omega_i\,.
\end{aligned}
\tag{30}
$$

Here the third equality defines an ion-mode wave-speed U_i, which is a factor ρ_p/ρ_i faster than the usual, single-fluid, Abbott-wave speed $U \equiv \partial g_{cak}/\partial v'$, as defined originally by Abbott (1980). Note that $U = \alpha\,g_{cak}/v' = \alpha\,v\,g(1+w)/vv' = \alpha\,v\,(1+1/w)$, which shows that this Abbott-wave speed is typically of order the wind speed [and indeed is exactly *equal* to the wind speed at the CAK critical point, where $w_c = \alpha/(1-\alpha)$]. The last two equalities – using the Sobolev length L to relate these wave speeds to corresponding growth rates Ω_i and Ω – will prove useful in the analysis to follow.

3.2.2.   Dispersion equation for long-wavelength perturbations

With these forms for the perturbed collisional and line-force terms, we are now in a position to derive a corresponding dispersion equation for the perturbation eigenmodes. Converting the two-component perturbation eqns. (26) and (27) into a two-by-two linear system and then taking the determinant of the coefficient array, we obtain a quadratic

dispersion relation for the complex frequency ω,

$$\omega^2 + B\omega + C = 0, \tag{31}$$

where the coefficients are given by

$$B = (kL + iq)\,\Omega_i + iq\Omega \approx k\,U_i + iq\,\Omega_i \tag{32}$$

and

$$C = ikL\,q\Omega\,\Omega_i\,. \tag{33}$$

The two solution modes are obtained trivially from the quadratic formula,

$$\omega_\pm = \frac{-1 \pm \sqrt{1 - 4C/B^2}}{2}\,B\,. \tag{34}$$

Noting that $4C/B^2 \sim \rho_i/\rho_p \ll 1$, we can approximate these two mode solutions with the simpler, explicit forms

$$\omega_+ \approx -\frac{C}{B} \approx \frac{-k\,U}{1 - ikL/q} \approx -k\,U \tag{35}$$

and

$$\omega_- \approx -B \approx -k\,U_i - iq\,\Omega_i \approx -iq\,\Omega_i\,. \tag{36}$$

The last approximations for each mode apply for these Sobolev-limit perturbations $kL \ll 1$ as long as one avoids pathological regimes for which $q \to 0$, that is, as long as the ion drift is not too strongly suprathermal (since then $q \sim -1/x_{pi}^2 \to 0$), or too near the drift speed ($x_{pi} = 0.968$) for the peak of the Chandrasekhar function (since then $G' \approx 0$ implies $q \approx 0$).

3.2.3. Solution eigenmodes for ion-coupling vs. ion-separation

To discern more clearly the character of these perturbation eigenmodes, let us next derive the associated eigenvectors, to obtain the phase and amplitude relations between the ion vs. passive-plasma velocity perturbations. From eqn. (26) we find

$$\delta v_i = \left(1 - \frac{i\omega}{q\Omega}\right)\,\delta v_p\,. \tag{37}$$

For the plus mode, application of eqn. (35) thus yields

$$\delta v_i^+ \approx \left(1 - \frac{ikU}{q\Omega}\right)\delta v_p^+ = \left(1 - \frac{ikL}{q}\right)\delta v_p^+ \approx +\delta v_p^+, \tag{38}$$

(using $kL \ll 1$, as above), while for the minus mode, use of eqn. (36) gives

$$\delta v_i^- \approx \left(1 - \frac{\Omega_i}{\Omega}\right) \delta v_p^- \approx -\frac{\rho_p}{\rho_i} \delta v_p^- . \tag{39}$$

From eqn. (38) we thus see that the plus solution represents an "ion-coupling" mode, for which the velocity perturbations for the ion and passive plasma are essentially identical. The frequency solution eqn. (35) shows moreover that this ion-coupling mode simply recovers the single-fluid, Abbott wave, which is marginally stable $[\mathrm{Im}(w_+) \to 0]$ and has an inward phase propagation at the Abbott speed, $\omega_+/k \approx -U$.

By contrast, eqn. (39) shows that the minus solution represents an "ion-separation" mode, for which the velocity perturbations for the ions vs. passive plasma have an *opposite* phase, with the ion velocity having a much higher amplitude. From eqn. (36) we see that the real part of the frequency implies that this mode has an essentially dispersionless (since $\mathrm{Re}(\omega_-) \sim k$) inward propagation at the fast 'ion-mode' Abbott speed, $U_i \approx 100\,U$.

Moreover, the large magnitude of the imaginary part of the frequency, $\mathrm{Im}(w_-) \approx -q\Omega_i$, can imply either a net damping ($q > 0$) or net amplification ($q < 0$) of this propagating wave mode. The damping applies in the high-density limit, with subthermal ion-drift-speed $x_{pi} < 1$; the amplification applies in the low-density limit, with suprathermal ion-drift-speed $x_{pi} > 1$. (See figure 1.) Applying eqn. (29) in eqn. (36), figure 5 plots the full drift-speed variation of the ion-separation damping or growth rate $\mathrm{Im}(\omega_-)$, scaled by the characteristic ion rate Ω_i. Note that this characteristic ion rate is *very* fast,

$$\Omega_i = \frac{\rho_p}{\rho_i}\,\Omega \approx 100\,\Omega \approx 100\,\frac{g_{cak}}{v_{th}} \approx 100\,\frac{vv'}{v_{th}} = 100\,\frac{v}{L} \approx 10^4\,\frac{v}{R_*} , \tag{40}$$

that is, typically a factor of 10,000 greater than a characteristic wind expansion rate!

3.2.4. *Weakness of spatial growth of ion separation in the long-wavelength limit*

Despite this extremely fast apparent *temporal* growth rate, the *spatial* growth of such long-wavelength, ion-separation perturbations generally remains quite modest, since this is given by ratio of the temporal growth to the (very fast) wave propagation speed,

$$\begin{aligned} \Lambda_i &\equiv \frac{\mathrm{Im}(\omega_-)}{-\mathrm{Re}(\omega_-)/k} \\ &\approx \frac{-q\,\Omega_i}{U_i} \\ &\approx \frac{-q}{L} . \end{aligned} \tag{41}$$
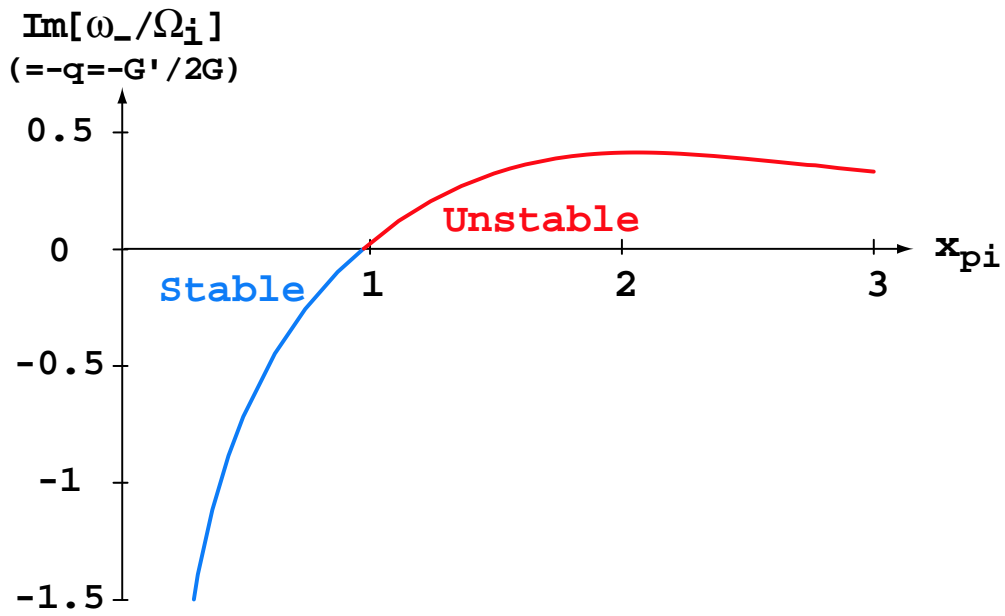
Fig. 5.— The imaginary part of the frequency for the ion-separation mode, Im(ω_-), scaled in units of the characteristic ion rate Ω_i, and plotted vs. the scaled ion drift speed x_{pi}. The negative values at subthermal drift speed indicate damping, while the positive values for suprathermal drift speeds indicate instability. For this case of long-wavelength perturbations $kL \ll 1$, the net rate for damping or amplification just depends on the negative of the collisional coupling strength, $-q$ [eqn. (29)], which in turn is proportional to the logarithmic derivative of the Chandrasekhar function [cf. figure 1].

Indeed, in the slow-acceleration, background solution of KK00, the Sobolev length $L \equiv v_{th}/v'$ can become quite large, implying a quite weak spatial growth.

Since the peak growth rate occurs at an ion drift speed of $x_{pi} \approx 2.05$, where there is a maximum in $-q \approx 0.41$ (figure 1), the spatial growth rate is limited to $\Lambda_i < 0.41/L = 0.41\, v'/v_{th}$, and indeed falls to zero at the collisional coupling maximum, where $q = 0$ and $v = v_{max}$. Thus, if we consider a long-wavelength perturbation applied to the KK00 slow-acceleration solution at a velocity that is Δv above v_{max}, then, in propagating back from the point of original perturbation to the stable region ahead of the collisional coupling maximum, the cumulative number of e-folds of amplification is less than

$$
\begin{aligned}
\max[\# \text{ e} - \text{folds}] &= 0.41 \int_{r}^{r_{max}} -dr/L \\
&= 0.41 \int_{r_{max}}^{r} dr\, v'/v_{th} \\
&= 0.41 \int_{v_{max}}^{v} dv/v_{th} \\
&= 0.41\, \Delta v/v_{th}\,.
\end{aligned}
\tag{42}
$$

Considering the near constancy of the velocity in slow-acceleration KK00 solutions, it thus seems that such solutions may not be too substantially disrupted by growth of such long-wavelength perturbations. Again, the physical reason is that, despite the very fast temporal amplification, the perturbation propagates rapidly inward, implying only a modest net amplification by the time it reaches the stable regime where $v < v_{max}$ and $q > 0$.

On the other hand, the spatial rate of *damping* of any perturbations in this stable regime can be quite large, since the positive value of q at low drift speeds is unbounded (figure 1), and since in the region before maximum coupling the flow acceleration is quite steep, implying a small Sobolev length L.

The derivation here of this ion-separation mode is a principle result of our analysis. The strong damping of the ion-separation perturbations for background flows with subthermal ion drift ensures that such high-density flows remain well-described by a single-fluid model, with mean properties set by the CAK model, and wave propagation given by the stable, Abbott mode. For suprathermal ion drift, we find that the ion-separation does become temporally very unstable, but with nonetheless a rather weak spatial growth.

It is, however, important to emphasize here that this ion-separation instability for such low-density flows applies even in the long-wavength, Sobolev limit. This is in contrast to the usual line-driven instability for single-fluid flows, which applies to small-scale perturbations with $kL \gtrsim 1$, and becomes entirely stable in the long-wavength, Sobolev limit $kL \ll 1$

(Abbott 1980; Owocki and Rybicki 1984, 1985). Let us thus next extend our two-component analysis to examine the nature of both the ion-coupling and ion-separation modes for such short-scale perturbations, with particular attention to determining whether there can be a stronger spatial amplification of ion separation at such short scales.

3.3. Generalization for Small-Scale Perturbations

3.3.1. The bridging law for the perturbed Ion line-force

For ion velocity perturbations δv_i with an arbitrary scale $1/k$ relative to the Sobolev length L, the perturbed ion line-force δg_i can be approximated by straightforward extension of the 'bridging law' derived for the single-compoent case (Owocki and Rybicki 1984, 1985)

$$\frac{\delta g_i}{\delta v_i} = \Omega_i \, \frac{ikL}{1 + ikL}, \tag{43}$$

where, for simplicity, we've just used the Sobolev length L to approximate the "bridging-length" that separates the behavior of short-scale perturbations from that in the large-scale, Sobolev limit.

3.3.2. Stabilty-dispersion analysis for arbitary scale perturbations

Let us thus apply this perturbed ion-line-force to derive a more general, two-component dispersion relation. The solutions again are given by the quadratic formula eqn. (34), but now with coefficients [cf. eqns. (32) and (33)]

$$B = iq\Omega + \left(iq + \frac{kL}{1 + ikL}\right)\Omega_i \approx \left(iq + \frac{kL}{1 + ikL}\right)\Omega_i \tag{44}$$

and

$$C = \frac{ikL}{1 + ikL} \, q\,\Omega\,\Omega_i \,. \tag{45}$$

Using as before $4C/B^2 \sim \rho_i/\rho_p \ll 1$, we again approximate the two eigenmode solutions in simple, explicit forms [cf. eqns. (35) and (36)],

$$\omega_+ \approx -\frac{C}{B} \approx \frac{-kL}{1 + ikL(1 - 1/q)} \, \Omega \tag{46}$$

and

$$\omega_- \approx -B \approx \left(-iq - \frac{kL}{1 + ikL}\right)\Omega_i \,. \tag{47}$$
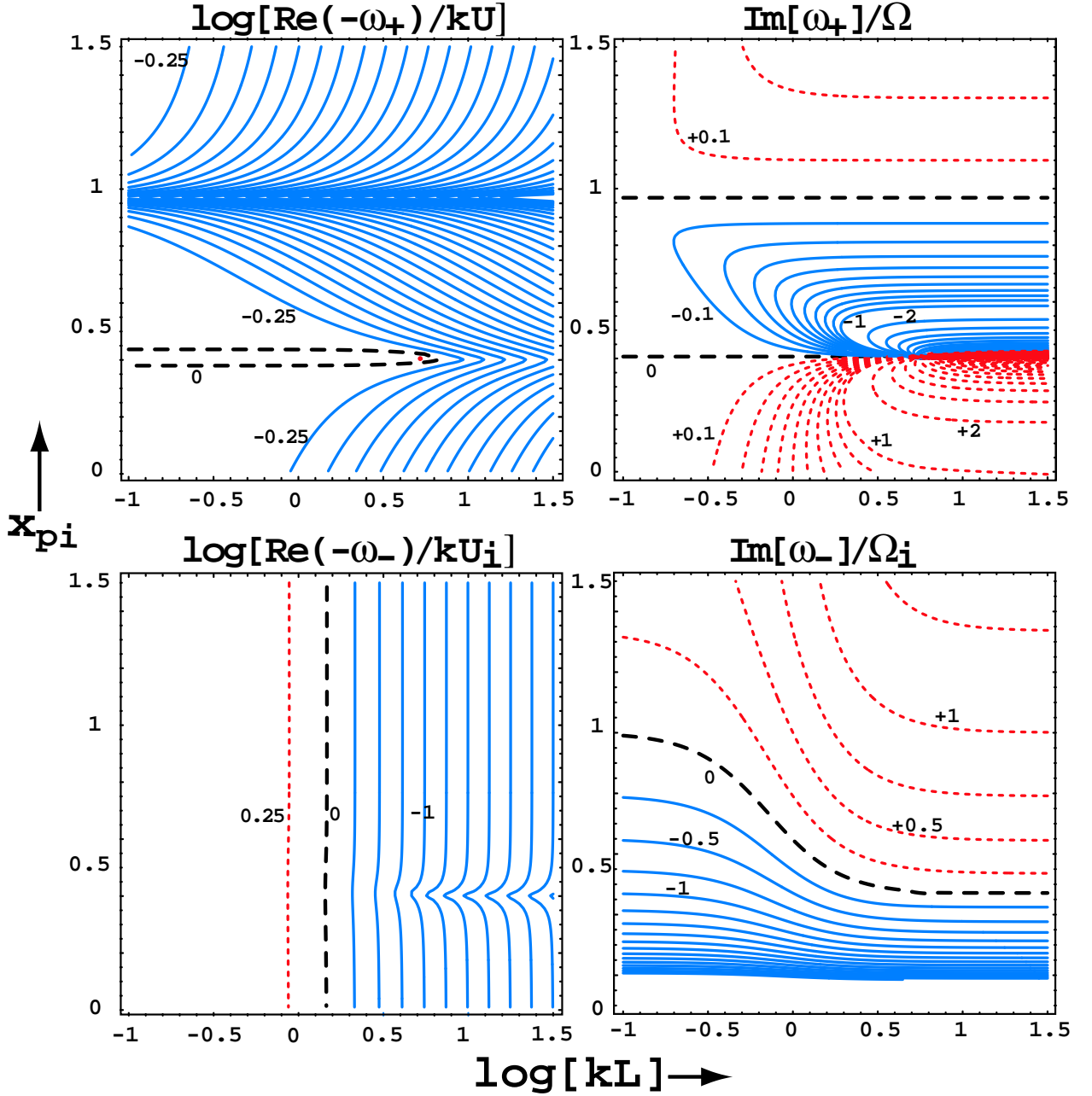
Fig. 6.— Frequency for the generalized dispersion solutions (46)-(47), plotted as contours vs. the thermally scaled ion drift speed x_{pi} [eqn. (6)] and the logarithm of the Sobolev-scaled perturbation-wavenumber, $\log[kL]$, with the upper and lower panels corresponding respectively to the ion-coupling (+) and ion-separation (-) modes. In the left panels the contours show the log of the phase speed, $\mathrm{Re}(\omega)/k$, scaled either by the Abbott speed U (top) or the faster ion-mode Abbott speed U_i (bottom). In the right panels the contours of $\mathrm{Im}(\omega)$ show the corresponding rates for wave damping (solid) or unstable growth (dotted), separated by the contour (dashed) for neutral stability [$\mathrm{Im}\,\omega = 0$], and scaled either by the characteristic rate Ω for the ion-coupling case (top), or by the faster ion-rate Ω_i for the ion-separation case (bottom). Contours are generally spaced equally in increments of 0.25 in the contoured variable, except in the upper right, for which the spacing jumps from 0.1 to 1, as labelled.

Applying these eigenfrequencies into eqn. (37), we obtain the corresponding generalized velocity eigenvector relations [cf. eqns. (38) and (39)] for the ion-coupling mode

$$\frac{\delta v_i^+}{\delta v_p^+} = 1 + \frac{ikL}{q(1 + ikL) - ikL} \,, \tag{48}$$

and the ion-separation mode

$$\frac{\delta v_i^-}{\delta v_p^-} = \left[-1 + \frac{ikL}{q(1 + ikL)} \right] \frac{\rho_p}{\rho_i} \,. \tag{49}$$

3.3.3. Eigenmode properties vs. wavenumber and ion-drift-speed

Figure 6 plots contours of the frequency solutions (46) and (47) as functions of both the perturbation wavenumber k and the ion drift speed x_{pi}, again using eqn. (29) to evaluate the coupling strength $q(x_{pi})$. The real parts of the frequency plotted in the left panels determine the phase speed while the imaginary parts plotted in the right panels determine the level of wave damping [$\mathrm{Im}(\omega) < 0$; solid curves] or unstable growth [$\mathrm{Im}(\omega) > 0$, dotted curves]. For completeness, we have plotted results for both the ion-coupling (top) and ion-separation (bottom) modes, though the latter is really of greater interest here. Moreover, as can be seen from figure 6, the behavior of the coupled modes is rather more complex, and so let's first concentrate on interpreting the separation mode results depicted in the bottom two panels.

From the lower left panel, we see that the phase propagation speed of this separation mode is (except near where $q \approx 1$) nearly independent of the drift speed x_{pi}, with a wavenumber variation that scales as $\mathrm{Re}(\omega_-)/k = -U_i/(1 + k^2 L^2)$. As noted in §3.2, for $kL \ll 1$ this gives fast inward propagation at the ion-mode speed U_i. But here we see that for $kL \gg 1$ this propagation speed declines as $U_i/(kL)^2$.

The lower right panel shows the key result for the damping or growth rates of this separation mode. As in the long-wavelength case, with increasing ion-drift speed, the strong damping for low drift (solid curves) first diminishes to marginal stability [$\mathrm{Im}(\omega) = 0$; dashed curve], and then becomes a strong amplification (dotted curves) for large drift-speeds. But note now that, for shorter-scale perturbations $kL > 1$, the transition to instability begins at lower, mildly subthermal drift speeds. In particular, in the short-wavelength limit $kL \gg 1$, the onset of instability occurs at $x_{pi} \approx 0.404$, for which $q(x_{pi}) \approx 1$.

Indeed, from the top panels we see this critical, $q = 1$ drift speed is one of two key separators (the other being the thermal drift speed $x \approx 0.968$, for which $q \approx 0$) for various domains in the real and imaginary parts of the coupled-mode frequency ω_+.

In the limit of strong coupling ($q \gg 1$, $x_{pi} \ll 1$), the ω_+ mode reduces to the standard instability "bridging-law" derived for the single-fluid case (Owocki and Rybicki 1984; 1985), with unstable growth at the rate Ω in the short-wavelength limit $kL \gg 1$, but (as found in §3.2.1) marginally stable, fast inward-wave propagation at the Abbott (1980) speed U in the long-wavelength, Sobolev limit $kL \ll 1$.

However, the top right panel of figure 6 shows that, for the higher x_{pi} (and lower q) that signify weaker collisional coupling, the short-scale ($kL \gg 1$) growth rate for this coupled mode is modified, and even becomes a net *damping* for $x_{pi} > 0.4$, for which $q < 1$. We thus see that the critical, $q = 1$ drift-speed separates the domain for the usual line-driven instabilty at $x_{pi} \ll 1$ from a stable region $0.4 \lesssim x_{pi} \lesssim 1$. This confirms speculations by Springmann (1993) that frictional dissipation might damp the line-driven instabilty for drift speeds approaching the thermal speed. But note that for large thermal speeds, $x_{pi} > 1$, the reduction in this frictional dissipation leads again to a net instability for this ion-coupling mode.

Finally, the top left panel again shows a rather elaborate behavior for the coupled-mode phase speed. In the strong coupling limit, $x_{pi} \ll 1$, this scales as $U/[1 + (kL)^2]$, and so declines as $U/(kL)^2$ at high wavenumbers $kL \gg 1$. But as the drift approaches the critical value at which $q = 1$, this decline becomes weaker, allowing the phase speed to remain relatively large, and even to exceed the usual value $\sim U$ in a small domain (too limited to show up in this contour plot) near $x_{pi} \approx 0.4$ and $\log(kL) \approx 0.6$. This then shifts to slower propagation for $x_{pi} \approx 1$, and then again to faster propagation for large ion-drift $x_{pi} > 1$.

3.3.4. *Strong spatial amplification of ion-separation for short-wavelength perturbations*

Overall, though, the most significant results of this extended perturbation analysis are in regards to properties of the ion-separation mode. First, note that small-scale perturbations actually become unstable to ion separation for mean flows with an ion drift of about a *half* the thermal-speed. This suggests that low-density flows could already become disrupted by ion separation even *before* reaching the maximal coupling that in steady-state models like KK00 leads to the turnover to low acceleration.

Moreover, in contrast to the long-wavelength results of §3.2, such short-scale ion-separation perturbations also generally have a quite strong spatial amplification. From eqn. (47), we find the spatial growth varies with the perturbation wavenumber k as

$$\Lambda_i \equiv \frac{\mathrm{Im}(\omega_-)}{-\mathrm{Re}(\omega_-)/k}$$
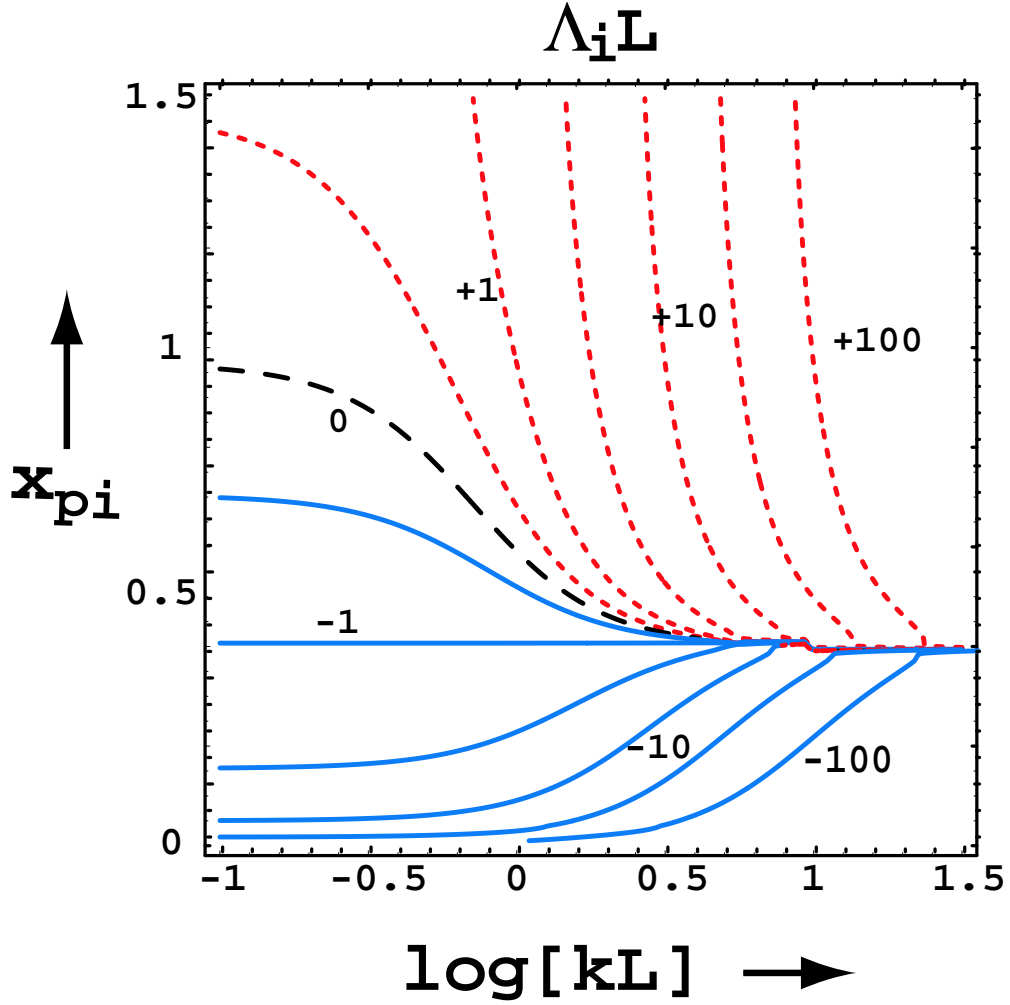
Fig. 7.— Contours of the spatial growth (dotted) or damping (solid) rate Λ_i [eqn. (50)] for the ion separation mode, scaled by the Sobolev length L, and plotted again vs. the ion drift speed x_{pi} and the logarithm of the scaled perturbation wavenumber kL. The positive and negative contours are each evenly spaced logarithmically with two contours per decade. The dashed contour shows the zero growth rate that separates unstable amplification ($\Lambda_i > 0$, dotted) from stable damping ($\Lambda_i < 0$, solid).

$$\approx \ \frac{-q + (1-q)(kL)^2}{L} \,. \tag{50}$$

Figure 7 plots contours of the scaled spatial growth rate $\Lambda_i L$ as a function of drift speed x_{pi} and the logarithm of the scaled wavenumber, $\log(kL)$. Note that in the long wavelength limit, $kL \ll 1$, we again recover the result of §3.2, namely only a weak spatial growth rate $\Lambda_i L \approx -q$. However, for short wavelengths, the decline in phase speed allows this spatial growth to become quite strong, scaling as $\Lambda_i L \approx (1-q)(kL)^2$ in the short-wavelength limit $kL \gg 1$.

Note, however, that the spatial propagation and growth derived in this way now only applies to each particular wavenumber perturbation. Unlike the nearly non-dispersive propagation of the long-wavelength case $kL \gg 1$, the phase propagation for arbitrary scales is now generally a strong function of the wavenumber, and so is highly dispersive. This means, for example, that one can no longer simply describe the group propagation of a locally confined perturbation, which consists of a Fourier composition of a large range of wavenumbers.

Generally, determining of the asymptotic properties of such localized perturbations requires an analyis of the perturbation Green's function, for example, using the 'pinch-point' method described by Bers (1983). Our preliminary calculations[3] indicate that the ion-separation instability found here is of the 'absolute' type, meaning that any localized perturbation should yield an exponential growth within the flow region it is introduced. This is to be contrasted with the 'advective' or 'drift' type of instability of the long-wavelength limit, for which the perturbation propagates away so rapidly that the region of introduction does not undergo a persistent exponential growth (Bers 1983; Owocki and Rybicki 1986).

Finally, we further emphasize that determining the ultimate outcome of this ion-separation instability will require a nonlinear analysis that includes complex plasma effects, e.g. two-stream instabilities, anomalous (collisionless) coupling, etc. Nonetheless, given the strong growth rates, it does seem likely that the ions could quickly become decoupled from the passive plasma. In this context, the counterintuitive lower-accelerations found in steady-state solutions appear indeed to be somewhat artificial, whereas the general intuition that the limited nature of collisional coupling should lead to ion runaway may in fact be a more accurate model of what could actually occur in such low-density, line-driven stellar winds.

---

[3] Through a straightforward extension of the analysis given in Appendix B of Owocki and Rybicki (1986), it can be shown that the Green's function for the ion-separation mode here follows the form given in their eqn. (B9), with just an added multiplicative factor $e^{-q\Omega_i t}$. Inspection of this form indicates that the flow is absolutely unstable to ion separation whenever $q < 1$.

4.   Summary and Future Work

In summary, let us list some key results and conclusions of the analyses in this paper:

1. We derive a simple but quite general scaling relation [eqn. (23)] for the stellar and wind parameters – gravity, wind temperature, mass loss rate and flow speed – at which a line-driven flow reaches the potential decoupling associated with suprathermal ion drift. This simple scaling is in good agreement with the conditions for which the detailed models of KK00 find instead a turnover to slow acceleration.

2. The KK00 slow-acceleration solutions arise physically from the lower ion line-force made possible by the lower collisional drag. As a result the overall steady flow switches to shallow-slope CAK solutions, for which the line-force mostly just needs to overcome the relatively weak retarding force of gravity.

3. In the ion momentum balance, the dominance of collisional drag over the ions' own inertia is characteristic of a subcritical flow, even beyond the usual CAK critical point. Moreover, such subcritical ion flow is consistent with the properties of a new "ion-mode Abbott-wave", which has a propagation speed that at its maximum is about a factor 100 faster than the usual Abbott-wave, and which thus can in principal propagate signals to the stellar base from anywhere in the wind.

4. But such fast ion waves are very strongly damped whenever the ion drift is substantially subthermal, and so they seem unlikely to be of much direct physical relevance for high-density, CAK-type winds.

5. On the other hand, in low-density winds with suprathermal ion drift these waves become unstable to ion separation, with a huge characteristic *temporal* growth rate.

6. For perturbations on a scale much larger than the Sobolev length, however, the fast propagation causes the *spatial* growth of this instability to remain rather small, implying the KK00 solution should not be too disrupted by such large-scale perturbations.

7. For perturbations on a scale at or below the Sobolev length, the onset of instability occurs even before the flow has reached this point of maximal coupling, roughly when the ion drift speed is about half a thermal speed. Moreover, the generally lower propagation speed now means that such small-scale perturbations also have very strong *spatial* growth.

8. Together these properties imply that low-density flows should become disrupted by ion separation even before reaching the point at which the KK00 steady-state analysis

predicts a turnover to slow acceleration, and this casts some doubt on the practical relevance of such steady, slow-acceleration solutions.

Within this context, however, it should be emphasized that our examination here of the physical origin of these slow acceleration solutions helps to affirm quite clearly that, within the steady-state assumption on which it was based, the KK00 analysis was entirely sound. These authors thus deserve considerable credit for being the first to rigorously *solve* a partially coupled, two-component extension of the classical CAK model, and for thereby uncovering an initially counterintuitive result that exposes hidden subtleties in the physics of line driving and collisional coupling.

There are, moreover, several potentially important caveats to our present conclusions that still need to be examined in future work. First, the stability analysis here is based on only a *two-fluid* model, treating the ions and passive plasma as distinct components that only interact via Coulomb collisions. We also assume a constant, common temperature for both these components. The first steps in extending this analysis might, therefore, parallel those taken in the follow-up steady-state analysis by KK01, namely to compute explicit energy equations for each component, and also to include the negatively charged electrons, and along with these the associated polarization electric field.

Even in a linear limit, such an extended perturbation analysis could begin to address key questions on the role of frictional heating in the onset of ion runaway. Moreover, with inclusion of perturbations in the polarization electric field, one could begin to examine the potential role of two-stream or other collective effects. In principle, these might contribute a damping that could reduce the level of instability. However, given the large growth rate found here for the ion-separation mode, complete negation of the linear instability by such plasma effects seems rather unlikely.

Nonetheless, the nonlinear outcome of this instability is still entirely uncertain. It could lead indeed to an effectively complete ion runaway, or might instead saturate at an ion drift of only a few thermal speeds, owing perhaps to dissipation from plasma wave modes excited by two-stream instabilities. Such collective effects have been quite extensively studied in the context of space plasma studies applied to, e.g. the solar wind or planetary magnetospheres, typically through quite elaborate numerical simulations (e.g., Scudder 1996).

In the context here of including the additional strong effect of radiative driving and the very rapid time scales of the associated ion-separation instability, analogous numerical simulations would be a formidable challenge to develop, and probably very computationally expensive to carry out. For example, since the strongest spatial ampflification occurs for perturbations at scales below the Sobolev length, one cannot rely on a local, Sobolev treat-

ment line-driving. Instead, as for the usual line-driven instability, one must apply *nonlocal*, integral treatment of the line-driving force. Moreover, as in these instability simulatons, the likely complexity of ion runaway simulation results will likewise pose a major challenge for conceptual interpretation.

On the other hand, as in that case, and even in the example here, such challenges for interpreting more realistically complex phenomena are often key to developing new insights and paradigms of simplification, and so lead to a deeper understanding of even the seemingly well-estabilished, basic model. Indeed, building on the thought-provoking results of KK00, the analysis here has led to discovery of a surprisingly rich new phenomenology of wave eigenmodes, and along the way also to some fresh perspectives on the quarter-century-old CAK paradigm. One can readily anticipate that still further twists, surprises, and new insights must await determined researchers seeking to understand better the subtle physical intricacies of flows driven by line scattering of radiation.

Appendix: Justification for the Neglect of Density Perturbations

We examine here the neglect of perturbations in density $\delta\rho_{p,i}$ in favor of velocity perturbations $\delta v_{p,i}$ in the analysis of §3. First, note that, in the momentum equations (1) and (2), the collisional force on each component depends on the density of the *other* component. Using the fact that in the mean flow the collision force $R_{p,i} \approx \rho_i g_i \approx \rho_p g_{cak}$ [eqns. (12) and (14)], we thus see that accounting for density perturbations requires additional terms of the form $(\delta\rho_i/\rho_i)g_{cak}$ and $(\delta\rho_p/\rho_p)g_i$ in respectively the perturbed momentum equations (26) and (27) for the passive-plasma and ion components. To compare these terms with the ones retained in eqns. (26) and (27), we need to relate the density and velocity perturbations. Using the perturbed mass conservation equations, which for both species imply

$$-i\omega\delta\rho + ik\,\rho\,\delta v = 0\,, \tag{51}$$

we immediately find $\delta\rho/\rho = \delta v/(\omega/k)$, and so the additional density perturbation terms can thus be written as $g_{cak}\delta v_i/(\omega/k)$ and $g_i\delta v_p/(\omega/k)$. Comparing these with the corresponding collisional perturbations $\delta v_i b/\rho_p$ and $\delta v_p b/\rho_i$, we find using eqn. (28) that they have a ratio

$$\frac{g_{cak}/(\omega/k)}{\alpha q\Omega} = \frac{v_{th}}{\alpha q\,\omega/k} \tag{52}$$

for both the passive-plasma and the ion momentum equations.

The real part of ω/k is just the phase velocity, and for the solutions derived in §3, this is either of order the Abbott speed U for the ion-coupling mode, or the still faster ion-mode Abbott-speed $U_i \approx 100U$ for the ion-separation mode. Since the Abbott-speed is itself on the order of the wind flow speed, $U \approx v$, we thus see that ratio in eqn. (52) is typically very small, of order $v_{th}/v \ll 1$, which thus justifies the neglect of these density perturbation terms in the analysis of §3.

If such terms are nonetheless included, the dispersion equation (cf. eqn. (31) becomes a quartic in frequency ω, and thus yields two new eigenmodes in addition to the coupled and separation modes discussed in §3. From direct solution of this quartic, we have confirmed, however, that both of these two additional solutions have typical frequencies of order $\omega \sim (v_{th}/v)\Omega$ or less, and thus are negligibly small compared to the dominant modes, for which either $\omega_+ \sim \Omega$ or $\omega_- \sim \Omega_i \sim 100\Omega$.

Finally, we note that we have also neglected such density perturbations in derivations of the perturbed ion-line-force δg_i. As noted by Owocki and Rybicki (1984), specifically in the discussion surrounding their eqn. (18), neglect of such terms in this context is consistent with the basic WKB approximation used in this analysis.

REFERENCES

Abbott, D. C. 1980, ApJ, 242, 1183

Abbott, D. C. 1982, ApJ, 259, 282

Bers, A. 1983, *Handbook of Plasma Physics*, Vol. 1, *Basic Plasma Physics*, A. Galeev and R. Sudan, eds., North Holland, Amsterdam, p. 451

Bromm, V., Kudritzki, R. P., & Loeb, A. 2001, ApJ, 552, 464

Castor, J. I., Abbott, D. C., & Klein, R. I. 1975, ApJ, 195, 157

Castor, J. I., Abbott, D. C., & Klein, R. I. 1976, *Physique des Mouvements dans les Atmospheres Stellaires*, R. Cayrel and M. Steinberg, eds., CNRS, Paris, 363

Dreicer, H. 1959, Physical Review , 115, 238

Feldmeier, A. & Shlosman, I. 2000, ApJ, 532, L125

Friend, D. B. & Abbott, D. C. 1986, ApJ, 311, 701

Gayley, K. G. 2000, ApJ, 529, 1019

Krtička, J. & Kubát, J. 2000, A&A, 359, 983

Krtička, J. & Kubát, J. 2001, A&A, 369, 222

Kudritzki, R. P. 2000, *The First Stars*, A. Weiss, T. Abel, V. Hill (eds.). Springer, p.127

Lamers, H. J. G. L. M. & Cassinelli, J. P. 1999, *Introduction to Stellar Winds*, Cambridge University Press, 1999.

Lamers, H. J. G. L. M. & Morton, D. C. 1976, ApJS, 32, 715

Lang, K. R. 1974, New York, Springer-Verlag New York, Inc., 1974. 760

Leer, E. & Holzer, T. E. 1980, J. Geophys. Res., 85, 4681

Lucy, L. B. & Solomon, P. M. 1970, ApJ, 159, 879

Owocki, S. P. & Puls, J. 1999, ApJ, 510, 355

Owocki, S. P. & Rybicki, G. B. 1984, ApJ, 284, 337

Owocki, S. P. & Rybicki, G. B. 1985, ApJ, 299, 265

Owocki, S. P. & Rybicki, G. B. 1986, ApJ, 309, 127

Pauldrach, A., Puls, J., & Kudritzki, R. P. 1986, A&A, 164, 86

Porter, J. M. & Drew, J. E. 1995, A&A, 296, 761

Porter, J. M. & Skouza, B. A. 1999, A&A, 344, 205

Scudder, J. 1996, J. Geophys. Res., 101, 13461

Springmann, U. W. E. 1992, Diplom Thesis, U. of Munich.

Springmann, U. W. E. & Pauldrach, A. W. A. 1992, A&A, 262, 515